Metabolic Engineering 10 (2008) 352–359

Contents lists available at ScienceDirect

Metabolic Engineering

journal homepage: www.elsevier.com/locate/ymben

Replacing *Escherichia coli* NAD-dependent glyceraldehyde 3-phosphate dehydrogenase (GAPDH) with a NADP-dependent enzyme from *Clostridium acetobutylicum* facilitates NADPH dependent pathways

Irene Martínez [a], Jiangfeng Zhu [a], Henry Lin [a,1], George N. Bennett [b], Ka-Yiu San [a,*]

[a] Department of Bioengineering, Rice University, Houston, TX, USA
[b] Department of Biochemistry and Cell Biology, Rice University, Houston, TX, USA

ARTICLE INFO

Article history:
Received 20 December 2007
Received in revised form
5 September 2008
Accepted 10 September 2008
Available online 23 September 2008

Keywords:
E. coli
Cofactor engineering
NADPH availability
NADP-dependent GAPDH

ABSTRACT

Reactions requiring reducing equivalents, NAD(P)H, are of enormous importance for the synthesis of industrially valuable compounds such as carotenoids, polymers, antibiotics and chiral alcohols among others. The use of whole-cell biocatalysis can reduce process cost by acting as catalyst and cofactor regenerator at the same time; however, product yields might be limited by cofactor availability within the cell. Thus, our study focussed on the genetic manipulation of a whole-cell system by modifying metabolic pathways and enzymes to improve the overall production process. In the present work, we genetically engineered an *Escherichia coli* strain to increase NADPH availability to improve the productivity of products that require NADPH in its biosynthesis. The approach involved an alteration of the glycolysis step where glyceraldehyde-3-phosphate (GAP) is oxidized to 1,3 bisphophoglycerate (1,3-BPG). This reaction is catalyzed by NAD-dependent endogenous glyceraldehyde-3-phosphate dehydrogenase (GAPDH) encoded by the *gapA* gene. We constructed a recombinant *E. coli* strain by replacing the native NAD-dependent *gapA* gene with a NADP-dependent GAPDH from *Clostridium acetobutylicum*, encoded by the gene *gapC*. The beauty of this approach is that the recombinant *E. coli* strain produces 2 mol of NADPH, instead of NADH, per mole of glucose consumed. Metabolic flux analysis showed that the flux through the pentose phosphate (PP) pathway, one of the main pathways that produce NADPH, was reduced significantly in the recombinant strain when compared to that of the parent strain. The effectiveness of the NADPH enhancing system was tested using the production of lycopene and ε-caprolactone as model systems using two different background strains. The recombinant strains, with increased NADPH availability, consistently showed significant higher productivity than the parent strains.

1. Introduction

Many redox enzymes catalyze synthesis reactions that lead to the formation of industrially important compounds. These reactions commonly require precursors and cofactors that could be provided by cells' primary metabolism. Reducing equivalents, such as NADPH or NADH, are usually required in large quantities. Whole-cell systems are able to supply and regenerate reducing equivalents, although the generation rate might be a limiting factor for reaching high yields and high productivities (Gunnarsson et al., 2004; San et al., 2002). The main source of NADPH in the cells is the pentose phosphate (PP) pathway where two molecules of the reduced cofactor are regenerated per glucose directed through that pathway. The tricarboxylic acid (TCA) cycle also regenerates NADPH but to a lower extent (Gunnarsson et al., 2004). To increase product yields, NADH levels have been manipulated in the past by overexpressing formate dehydrogenase in *E. coli* (Berrios-Rivera et al., 2002a–c, 2004; Ernst et al., 2005; Hummel, 1997). On the other hand, NADPH levels have been manipulated in *Saccharomyces cerevisiae* by overexpressing the malic enzyme (Moreira dos Santos et al., 2004; Sanchez et al., 2006) or the $NADP^+$-dependent D-glyceraldehyde-3-phosphate dehydrogenase (NADP-GAPDH) from *Kluyveromyces lactis* (Verho et al., 2002, 2003); and in *E. coli* by forcing the carbon flow through the PP pathway by knocking out the phosphoglucoisomerase gene (*pgi*) (Kabir and Shimizu, 2003a), although this approach resulted in growth deficiency. Another approach to increase NADPH availability in *E. coli* has been the overexpression of the endogenous pyridine nucleotide transhydrogenase (UdhA)

* Corresponding author.
E-mail address: ksan@rice.edu (K.-Y. San).
[1] Current address: Amgen Inc, Thousand Oaks, CA, USA.

1096-7176/$ - see front matter © 2008 Elsevier Inc. All rights reserved.
doi:10.1016/j.ymben.2008.09.001

(Sanchez et al., 2006), which catalyzes a reversible reaction where the reducing power can be interchanged between NADH and NADPH ($NADH + NADP^+ \overset{UdhA}{\longleftrightarrow} NAD^+ + NADPH$), therefore if NADPH is consumed, the enzyme has the potential to replenish it.

In the present work, *E. coli* primary metabolism, specifically one glycolysis step, has been modified to increase product yields in NADPH-dependent synthesis systems. The endogenous *gapA* gene, encoding for a NAD-dependent GAPDH, was knocked out and the *gapC* gene from *C. acetobutylicum*, encoding a NADP-dependent GAPDH, was overexpressed to generate NADPH instead of NADH in the oxidation of GAP during glycolysis. This modification increases the amount of NADPH produced through the glycolysis pathway maintaining such primary pathway functioning producing metabolites, precursors and energy. The modified strain was characterized by metabolic flux analysis (MFA) and the effect of the alterations in product yield and productivity were assessed using the synthesis of lycopene and ε-caprolactone as model systems. The genes required for the synthesis of these compounds were heterologously expressed in the recombinant *E. coli*.

Lycopene is a red-colored carotenoid naturally found in vegetables (tomato) and fruits. This compound is a commercially important product widely used as antioxidant, colorant and precursor of other carotenoids. Recent studies have suggested that the ingestion of lycopene could reduce the risk of certain cancers (including prostate, lung and breast cancers) (Agarwal and Rao, 2000), prevent atherosclerosis and cardiovascular heart diseases (Rao and Agarwal, 2000) as well as enhance immune system response (Agarwal and Rao, 2000; Bose and Agrawal, 2007; Minorsky, 2002; Rao and Agarwal, 2000; Stacewicz-Sapuntzakis and Bowen, 2005). Lycopene has been produced in *E. coli* by means of the non-mevalonate pathway expressing the lycopene synthetic operon *crtEBI* from *Erwinia herbicola* (Alper et al., 2005; Cunningham et al., 1994; Vadali et al., 2005). The biosynthesis requires GAP, pyruvate and a high amount of NADPH (16 molecules of NADPH per molecule of lycopene) (Alper et al., 2005) (Fig. 1).

Baeyer–Villiger (BV) reactions are very important in chemical and pharmaceutical industries. They involve the oxidation of aliphatic and cyclic ketones to produce esters and lactones, respectively. The traditional BV chemical process involves the use of peroxyacids or hydrogen peroxide and a transition metal catalyst. This process has low stereoselectivity, possible high recovery costs and it is detrimental to the environment. On the other hand, many oxidoreductases have been studied for their ability to catalyze environmentally friendly enantio-, chemo- or regioselective reactions to produce a variety of compounds with high optical purity, extremely important for chemical and pharmaceutical applications. In particular, monooxygenases have been found to be highly stereoselective (Schulz et al., 2005). These enzymes use molecular oxygen and require NAD(P)H. Baeyer–Villiger monooxygenases (BVMOs) are found in a wide variety of organisms such as *Acinetobacter* sp. (Donoghue et al., 1976), *Arthrobacter* (Kyte et al., 2004), *Comamonas*, *Rhodococcus*, *Xanthobacter* (Van Beilen et al., 2003), *Nocardia* (Donoghue et al., 1976), *Brevibacterium* (Mihovilovic et al., 2003), and *Pseudomonas fluorescens* (Kirschner et al., 2007), among others. These enzymes have been used in isolated form or as whole-cell biocatalysts. Whole-cells of their native organism or recombinant forms of *E. coli* or *S. cerevisiae* have also been studied (Baldwin and Woodley, 2006; Lee et al., 2005; Walton and Stewart, 2002, 2004). BVMOs are able to accept a wide range of substrates with variable stereoselectivity. In particular, cyclohexanone monooxygenase (CHMO) from *Acinetobacter* sp. NCIB 9871 has been shown to oxidize thioethers and cyclohexanones into sulfoxides and δ- and ε-caprolactones with high enantioselectivity (>95%) (Chen et al., 1999; Lee et al., 2005; Stewart et al., 1996; Walton and Stewart, 2002). ε-caprolactone is an important intermediate in the manufacture of polyurethane adhesives, thermoplastics (Lee et al., 2005), resins for surface coatings and synthetic leather and fabrics. BVMO reactions require stoichiometric amounts of reducing equivalents that must be regenerated, which adds complexity and cost to the system. In this work, we used cyclohexanone monooxygenase (CHMO) from *Acinetobacter* sp. to study the effect of our recombinant *E. coli* in ε-caprolactone yield and productivity (Fig. 2). The recombinant *E. coli* in this case acts exclusively as a regenerator of NADPH using glucose as energy source. This reaction gives a more direct measure of the NADPH availability in our system. One mole of NADPH is consumed per mole of ε-caprolactone produced.

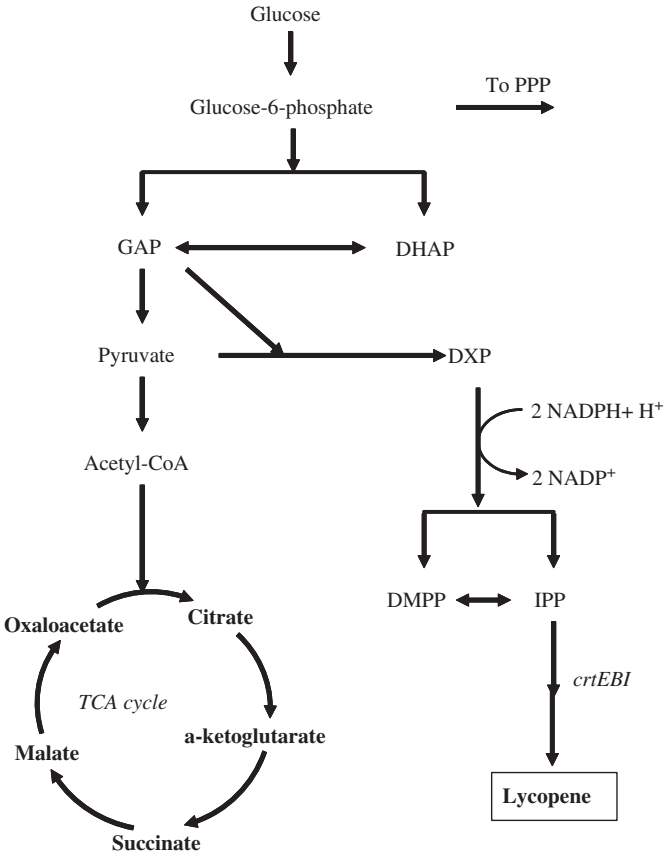

Fig. 1. Lycopene synthesis pathway in recombinant *E. coli*. GAP: glyceraldehyde-3-phosphate, DHAP: dihydroxyacetone-3-phosphate, DXP: deoxyxylulose 5-phosphate, DMPP: dimethylallyl pyrophosphate, IPP: isopentenyl phosphate, PPP: PP pathway.

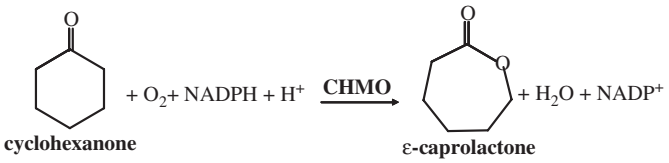

Fig. 2. Synthesis of ε-caprolactone in recombinant *E. coli* expressing cyclohexanone monooxygenase (CHMO) from *Acinetobacter* sp.

2. Materials and methods

2.1. GAPDH assay

E. coli GAPDH catalyzes the conversion of glyceraldehyde-3-P (GAP) to 1,3-bisphosphoglycerate (1,3BPG) using NAD^+ or $NADP^+$

as a cofactor, depending on the enzyme origin. GAPDH activity was measured using method adapted from Iddar (Iddar et al., 2002). To 200 μl of crude extract, 250 μl of 200 mM tricine buffer (pH 8.5), 300 μl of mercaptoethanol, 100 μl of 10 mM $NAD(P)^+$ and 50 μl DI water were added, and finally 100 μl of 10 mM GAP were added just prior to measurement. Enzyme activity was followed by monitoring change in absorbance at 340 nm. The extinction coefficient used was 6.22 $mM^{-1}\,cm^{-1}$.

2.2. Bacterial strains and plasmids

Strains and plasmids used in this work are listed in Table 1. The W3CG strain was generously donated by the *E. coli* Genetic Stock Center. Two *gapA* mutant strains with different *E. coli* genetic backgrounds (MG1655 and BL21(DE3)) were constructed by P1-Phage transduction using *E. coli* W3CG (*E. coli* W3110 Δ*gapA*, Tc^R) as the donor strain (Ganter and Pluckthun, 1990). The MG1655 Δ*gapA* strain harboring the plasmid pK19-Lyco encoding for *crtE*, *crtI* and *crtB* genes from *E. herbicola* was used for the lycopene production experiments. The BL21(DE3) *E. coli* strain contains the gene encoding for the T7 RNA polymerase, used for expression of genes under the T7 promoter. The plasmid pMM4, used for ε-caprolactone synthesis, encodes for the CHMO from *Acinetobacter* sp. NCIB 9871 gene under the T7 promoter, then, this host strain expressing the T7 RNA polymerase was constructed for CHMO expression and thus ε-caprolactone biosynthesis. The plasmid pMM4 was kindly provided by Dr. Stewart (University of Florida).

The *E. coli gapA* mutant strains were selected on LB agar plates containing 15 mg/L tetracycline and the mutation was confirmed by GAPDH assay and strain inability to grow on minimal medium containing glucose as the sole carbon source (6 g/L Na_2HPO_4, 3 g/L KH_2PO_4, 0.5 g/L NaCl, 1 g/L NH_4Cl, 0.1 mM $CaCl_2$, 1 mM $MgSO_4$, 15 g/L agar, 20 mM glucose). The *E. coli gapA* mutants showed negligible GAPDH activity (data not shown).

The *gapC* gene, encoding for the NADP-dependent GAPDH, was amplified by PCR from *C. acetobutylicum* chromosomal DNA. The primers 5′-GCTCTAGAGCATGAGGTAGTTAGAATGGC-3′ and 5′-CGGGATCCCGCAAATTAATTAATGAGCGC-3′ were used in the PCR reaction. The PCR product (about 1 kb) was digested with XbaI and BamHI (restriction sites are underlined in the primer sequences) and cloned into plasmid pDHC29 (Cm^R). One plasmid which showed a high level of GAPDH activity (data not shown) was selected and was designated as plasmid pHL621.

Table 1
List of strains and plasmids used in this work

	Relevant genotype	Reference
E. coli strains		
MG1655	Wild type *E. coli*	ATCC 47076
BL21(DE3)	For T7-promoter expression	Invitrogen
W3CG	W3110 *gapA*	Ganter and Pluckthun (1990)
MBS100M	MG1655 *gapA*	This study
MBS100B	BL21(DE3) *gapA*	This study
Plasmids		
pDHC29	Cloning vector, Cm^R	Phillips et al. (2000)
pHL621	*gapC* from *C. acetobutylicum* in pDHC29, Cm^R	This study
pAC-LYC	*crtE*, *crtI*, *crtB* genes from *E. herbicola* in pACYC184, Cm^R	Cunningham et al. (1994)
pK19	Cloning vector, Km^R	Pridmore (1987)
pK19-Lyco	*crtE*, *crtI*, *crtB* genes from *E. herbicola* in pK19, Km^R	This study
pMM4	CHMO gene from *Acinetobacter* sp. NCIB 9871 in pET22b(+), Ap^R	Chen et al. (1999)

The *crtEBI* operon encoding for lycopene synthesis enzymes together with the native promoter were cloned from pAC-Lyc plasmid, Cm^R (Cunningham et al., 1994) into the kanamycin resistant pK19 vector (Pridmore, 1987) using HindIII and EcoRI restriction sites. The new plasmid, pK19-LYC, is compatible with pHL621 (Cm^R). The pAC-Lyc plasmid was kindly donated by Dr. Francis Cunningham, Jr. (Botany Department, University of Maryland, College Park, MD).

2.3. Metabolic flux analysis

2.3.1. Continuous culture

Glucose-limited chemostat cultures were made at a dilution rate of $0.35 \pm 0.01\ h^{-1}$ using 20 mM of glucose as a sole carbon source. The medium used was a minimal media containing (per liter) 7 g Na_2HPO_4, 3 g KH_2PO_4, 0.5 g NaCl, 1 g NH_4Cl, 6 mg thiamine, 1 mM $MgSO_4$, 0.1 mM $CaCl_2$ and 35 μg/ml chloramphenicol. A 1-L bioreactor (BioFlo 110, New Brunswick Scientific Edison, NJ) was used for the cultures and the working volume was maintained at 600 ml. The pH value was maintained at 7.0 ± 0.04 by titrating with 3 M NaOH and 1.5 M of HNO_3. The temperature was maintained at 37 °C. The aerobic culture condition was controlled by purging the culture broth in the bioreactor with air and maintaining the agitation speed at 285 rpm. The gas flow rate was controlled at 2 L/min.

2.3.2. Analytical procedures

Cell dry weight was determined from cell pellets of 100-ml culture aliquots that were centrifuged for 10 min at 4 °C and $5{,}000 \times g$, washed twice with 0.15 M NaCl, and then dried at 50 °C until the weight was constant. Culture broth samples were centrifuged for 3 min at $13{,}000 \times g$ in an AccuSpin™ micro centrifuge. The supernatant was filtered through a 0.2 μm syringe filter and stored chilled for HPLC analysis. The extracellular metabolites and glucose were quantified using an HPLC system (Shimadzu Scientific Instruments, Columbia, MD) equipped with a cation-exchange column (HPX-87H, BioRad Labs, Hercules, CA), a differential refractive index detector (Waters, Milford, MA) and a UV–VIS detector (SPD-10A, Shimadzu Scientific Instruments, Columbia, MD). A mobile phase of 2.5 mM H_2SO_4 solution at a 0.6 ml/min flow rate was used and the column was operated at 55 °C (Sanchez et al., 2005; Yang et al., 1999).

2.3.3. Labeling experiments and metabolic flux analysis

We assumed that the steady state was reached after seven volume changes when the optical density at 600 nm remained constant for at least three residence times. Labeling experiments were started after the cultures reached the steady state. The unlabeled feeding media was replaced by an identical medium containing 16 mM unlabeled glucose, 2 mM [U-^{13}C] glucose, and 2 mM [1-^{13}C] glucose. Biomass samples were taken at the end of the chemostat cultures for GC/MS detection. Cells in 50 ml of culture were harvested by centrifugation for 10 min at 4 °C and $5{,}000 \times g$. The cell pellets were washed three times with 20 mM Tris-HCl (pH 7.6) and resuspended in ca. 6 ml of 6 M HCl. The mixture was hydrolyzed for 12 h at 105 °C and the hydrolysate was filtered through a 0.2 μm pore-size filter and evaporated to dryness. There were 16 proteinogenic amino acids in the resulting hydrolysate, since cysteine and tryptophan were oxidized and asparagine and glutamine were deaminated during the HCl hydrolysis (Szyperski, 1995). The dried hydrolysates were derivatized and measured using GC-MS as previously described (Zhu et al., 2006).

To quantitatively estimate the metabolic flux analysis in the main metabolic pathways, a metabolic network was constructed

(Fig. 3) including glycolysis, PP pathway, TCA cycle and fermentative pathways. Some metabolic pools like pentose phosphates, succinyl-CoA and succinate (SUC), isocitrate (ICT) and citrate, were combined to simplify the network. The reactions through phosphoenolpyruvate carboxylase (Pepc) and phosphoenolpyruvate carboxykinase (Pck) were combined into a bi-directional reaction, and the reaction toward oxaloacetate (OAA) production was used as the positive direction. Since glucose was used as a sole carbon source, we did not consider the glyoxylate shunt and Entner-Doudoroff pathway for the flux estimation (Stephanopoulos et al., 1998). The cell composition was assumed to be the same in the experimental strains and it was derived from Neidhardt et al. (1990).

The metabolic flux distributions in the steady states were estimated using a newly developed computer program written in MATLAB (Version 7.0, The Mathworks Inc.) based on GC-MS measurements (Zhu et al., 2006). The flux estimation was made using a similar idea as was previously described (Schmidt et al., 1997; Wiechert et al., 1997; Zhao and Shimizu, 2003). Briefly, by giving some arbitrary values for the free fluxes, different sets of metabolic flux distributions can be determined based on stoichiometric constrains. Then the GC-MS data can be simulated based on the estimated flux distribution and the labeling pattern of the feeding glucose. The best fit set of flux distribution can be elected by comparing the simulated GC-MS data and the experimental GC-MS data. The reversible reaction fluxes were converted into net fluxes and exchange coefficients (within the range of [0,1]) as previously described (Wiechert and de Graaf, 1997). Isotopomer mapping matrices were developed based on atom mapping matrices (Schmidt et al., 1997; Zupke and Stephanopoulos, 1994) to trace the isotopomer changes in the reactions, and they were used for isotopomer balances based on different sets of metabolic flux distribution. The isotopomer distributions in the amino acids were deduced from the isotopomer distributions of their precursor metabolites. Then the GC-MS signals were simulated using the isotopomer distributions of amino acids. The flux solutions were evaluated by comparing the simulated data with the experimental data. The GC-MS data was corrected for the presence of naturally labeled H, C, N, O, Si, P, and S elements in the amino acids and derivatization reagent before they were used for flux analysis (Lee et al., 1992; van Winden et al., 2002). The best-fit sets of flux distributions were found using the genetic and direct search toolbox in MATLAB. The statistical analysis was made using a Monte Carlo approach (Schmidt et al., 1999; Zhao and Shimizu, 2003).

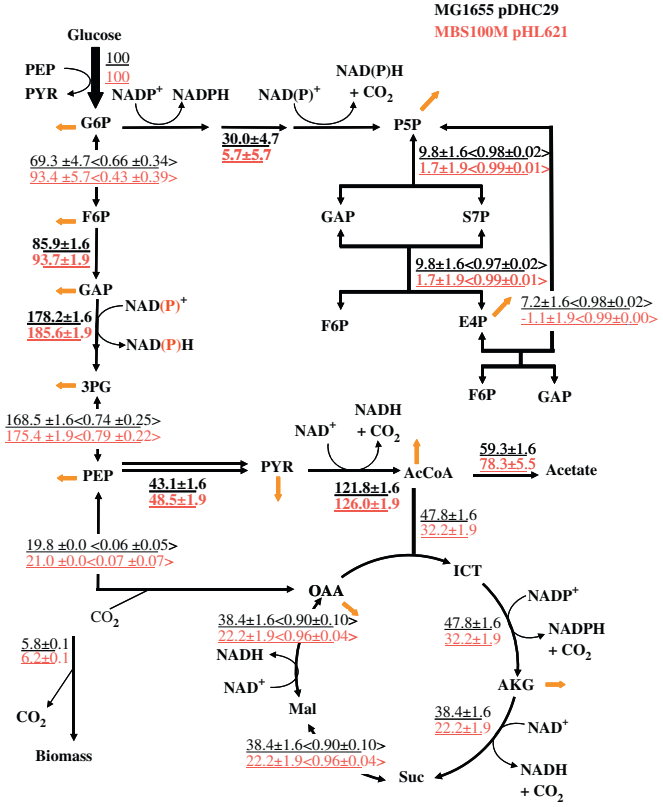

Fig. 3. Metabolic flux distribution in *E. coli* MG1655 pDHC29 (control) and *E. coli* NADH-GAPDH mutant strain overexpressing a NADPH-GAPDH from *C. acetobutylicum* (MBS100M pHL621) are shown in the top and bottom rows, respectively. The values in brackets (〈 〉) represent the exchange coefficients of the fluxes. The orange arrows represent the precursors for biomass formation. The abbreviation used in this figure can be found in Appendix A.

2.4. Experimental description

2.4.1. Lycopene experiments

Shake flask experiments were performed using 250 mL shake flasks containing 50 mL LB (10 g/L tryptone, 5 g/L yeast extract, 10 g/L NaCl) or 2YT (16 g/L tryptone, 10 g/L yeast extract, 5 g/L NaCl) medium supplemented with 20 g/L of glucose and 100 mM phosphate buffer (pH 7.0). Chloramphenicol (34 mg/L) and kanamycin (50 mg/L) were added to maintain plasmid stability. The cultures were inoculated with 1% (vol/vol) of overnight culture and grown at 30 °C and 250 rpm. After 24 h, the lycopene concentration was determined using established protocols (Kim and Keasling, 2001; Vadali et al., 2005; Alper and Stephanopoulos, 2008). Briefly, 10 mL samples were centrifuged at 13,000 × *g* for 5 min and the pellets were washed once with DI water. The cells were resuspended in 5 mL of acetone and incubated at 55 °C for 15 min in the dark with intermittent vortexing, to extract the lycopene accumulated in the cells. The samples were centrifuged at 13,000 × *g* for 10 min and the supernatant absorbance was read at 475 nm. To determine lycopene concentration, a calibration curve was constructed using lycopene standard (Sigma, St. Louis, MO). The extinction coefficient (ε) used was 2.59 cm L/mg.

2.4.2. CHMO experiments

Cultures of MBS100B (pHL621+pMM4) and BL21(DE3) (pDHC29+pMM4) were streaked on LB plates containing 34 mg/L chloramphenicol and 100 mg/L ampicillin and grown at 37 °C. Single colonies from these plates were used to inoculate 5 ml of liquid LB medium containing 34 mg/L chloramphenicol and 100 mg/L ampicillin. After shaking overnight at 250 rpm and 37 °C, 4 mL were used to inoculate 400 mL of LB medium supplemented with 34 mg/L chloramphenicol and 100 mg/L ampicillin. The cells were grown at 250 rpm and 37 °C until OD_{600} reached 0.6–1.0; at this time 0.1 mM IPTG (final concentration) was added. The culture was continuously incubated until it reached late exponential/stationary phase. The cells were centrifuged at 12,000 × *g* and 4 °C for 5 min. The pellet was re-suspended to an OD_{600} of 2.0 in 20 ml of non-growing medium (12.8 g/L Na_2HPO_4, 3.0 g/L KH_2PO_4, 0.5 g/L NaCl, 2 mM $MgSO_4$, 0.1 mM $CaCl_2$, 0.4% glucose, 30 mM cyclohexanone, and appropriate amount of antibiotics). The flasks were incubated at 250 rpm and 32 °C. Samples (3 ml each) were centrifuged, filtrated and then analyzed by HPLC. Cyclohexanone and ε-caprolactone were analyzed using a HPLC column Luna 5 μm C18(2) 100A, 250 × 4.6 mm (Phenomenex, Torrance, CA), 30–70% acetonitrile-water mobile phase at a flow rate of 1 ml/min. Column, RI and UV detectors temperature was 40 °C. The retention times for cyclohexanone and ε-caprolactone were 8.0 and 5.28 min, respectively.

Glucose concentration was analyzed as described previously (Sanchez et al., 2005; Yang et al., 1999).

3. Results

3.1. Metabolic flux analysis

3.1.1. Growth parameters

The maximum specific growth rate (μ_{max}) of the cultures was determined in shake flasks experiments. The μ_{max} for the control strain (MG1655 pDHC29) and the NAD$^+$-GAPDH *E. coli* mutant strain overexpressing the NADP$^+$-GAPDH from *C. acetobutylycum* (MBS100 M pHL621) were 0.48 and 0.38 h^{-1}, respectively. As such, the glucose-limited aerobic chemostat cultures were carried out at a dilution rate of 0.35 h^{-1}. The biomass yields and specific glucose uptake rates of the two strains are summarized in Table 2. It can be seen that the biomass yields and the specific glucose utilization rates were similar in the two experimental strains, while the *gapA* mutant strain showed a significantly higher specific acetate excretion rate compared to that of the control strain ($P<0.05$). The carbon recoveries were calculated from the biomass and fermentative metabolite production determined by experimental measurements, and the CO_2 production was derived from the flux distributions (Fig. 3) of the experimental strains. The carbon recovery values showed in Table 2 confirmed our network assumptions.

3.1.2. Metabolic flux analysis results

The metabolic flux distributions in the cultures of the two experimental strains were estimated based on C-13 labeling experiments. As shown in Fig. 3, the flux partitioning at glucose 6-phosphate (G6P) node was significantly affected by the genetic manipulation which replaced the native NAD-dependent *gapA* gene with an exogenous NADP-dependent *gapC*. The flux through glycolytic pathway was increased about 35% in the mutant strain compared to that in the control strain. Correspondingly, the flux through the oxidative PP pathway, one of the main pathways used to produce NADPH in *E. coli*, was reduced to less than 20% of that in the control strain. The activities of the non-oxidative PP pathway reactions were also reduced in the metabolic engineered strain (Fig. 3).

The flux through GAPDH was slightly higher in the mutant strain than that in the control strain. However, the flux difference in this reaction is much smaller than that at the G6P node. Considering the lower value of the transaldolase net flux and the negative value of the transketolase net flux in the mutant strain, the relatively higher GAPDH flux was mainly caused by the flux distribution at the G6P node.

Another important branch point is the Acetyl Coenzyme A (AcCoA) node. The mutant strain converted ca. 25.6% of AcCoA into the TCA cycle, relatively lower than the 39.2% in the control strain (Fig. 3). Therefore, less NADPH was produced from the reaction through isocitrate dehydrogenase in the mutant strain than the control. As a result of lower TCA cycle flux, the mutant strain excreted more acetate than the control strain.

The flux through phosphoenolpyruvate carboxylase (Pepc) was used to supplement the oxaloacetate (OAA) pool to sustain the TCA cycle and provide precursor for biomass synthesis. The relatively higher ($P<0.05$) Pepc flux was consistent with higher flux toward biomass in the mutant strain than that in the control.

3.2. Lycopene production experiments

The cell growth of the mutant *E. coli* strain was comparable and actually slightly higher ($\approx$ 6%) than the control, showing that no growth impairment was detected. The use of 2YT medium resulted in ca. 19% increase in cell concentration for both strains (Fig. 4). A significant difference was found in lycopene production between the two strains. The mutant strain produced lycopene equivalent to 2.5-fold that of the control in concentration (Fig. 5) and 2.4-fold when expressed as specific lycopene production (Fig. 6). The specific lycopene production was higher with the LB medium than with the 2YT, although that difference was less significant for the final lycopene concentrations. These results showed that the modified *E. coli* strain was able to increase lycopene yield.

3.3. ε-caprolactone production experiments

The mutant strain MBS100B (pHL621+pMM4) showed higher ε-caprolactone yield that the control, 2.97, compared to 1.72 mol ε-caprolactone/mole glucose (Table 3). One mole of NADPH is consumed per mole of ε-caprolactone produced (Fig. 2); therefore

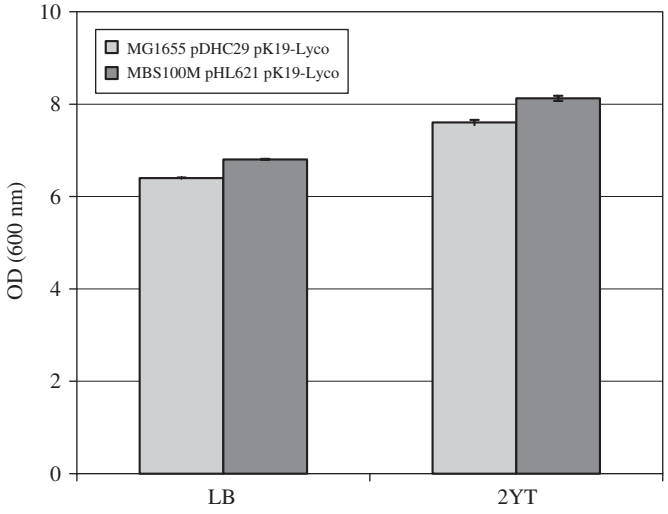

Fig. 4. Cell growth of control (MG1655 pDHC29 pK19-Lyco) and modified *E. coli* (MBS100M pHL621 pK19-Lyco: *E. coli* NADH-GAPDH mutant strain overexpressing a NADPH-GAPDH from *C. acetobutylicum*) strains after shake flask culture under aerobic conditions using LB or 2YT medium supplemented with 20 g/L of glucose for 24 h at 30 °C and 250 rpm. The data shown is the average of three replicate experiments where the error bars represent the standard deviation. Both strains express the pK19-Lyco plasmid containing the genes for lycopene biosynthesis (See Table 1).

Table 2
Growth parameters determined for the chemostat cultures of a NADH–GAPDH *E. coli* mutant strain overexpressing a NADPH–GAPDH from *C. acetobutylicum*

Strain	Biomass yield (g/g glucose)	Specific rates (mmol/g DCW/h)		C balance (%)
		Glucose consumption	Acetate production	
MG1655 pDHC29 (control)	0.27 ± 0.01	6.15 ± 0.14	3.64 ± 0.08	103 ± 5
MBS100M pHL621 (MG1655 Δ*gapA gapC*$^+$)	0.29 ± 0.02	6.18 ± 0.44	4.98 ± 0.39	96 ± 3

Errors were calculated based on at least three measurements.

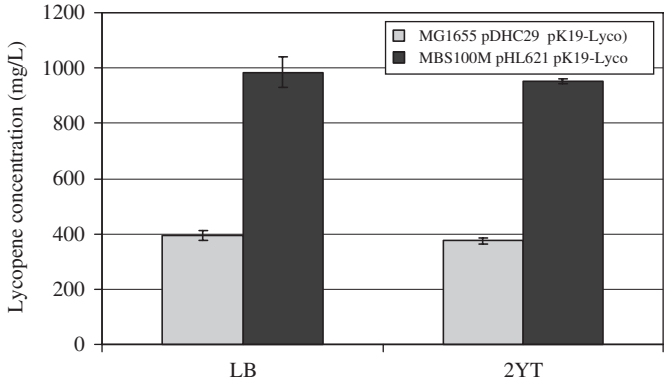

Fig. 5. Lycopene concentration, based on culture volume, of control (MG1655 pDHC29 pK19-Lyco) and modified *E. coli* (MBS100M pHL621 pK19-Lyco: *E. coli* NADH-GAPDH mutant strain overexpressing a NADPH-GAPDH from *C. acetobutylicum*) strains after shake flask culture under aerobic conditions in LB or 2YT medium supplemented with 20 g/L of glucose for 24 h at 30 °C and 250 rpm. The data shown are the average of three replicate experiments where the error bars represent the standard deviation. Both strains express the pK19-Lyco plasmid containing the genes for lycopene biosynthesis (see Table 1).

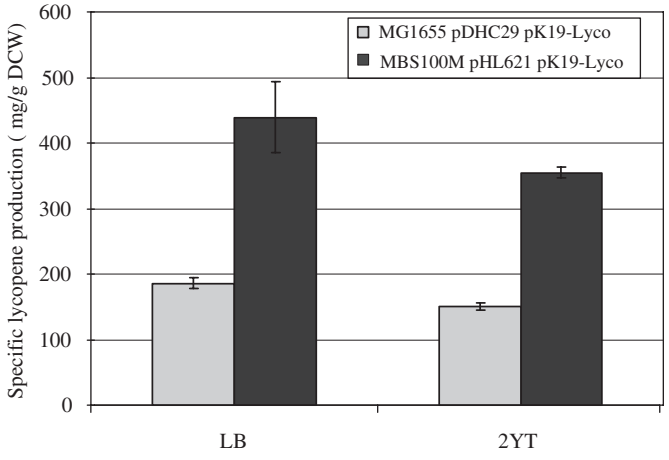

Fig. 6. Specific lycopene production, based on dry cell weight (DCW), of control (MG1655 pDHC29 pK19-Lyco) and modified *E. coli* (MBS100M pHL621 pK19-Lyco: *E. coli* NADH-GAPDH mutant strain overexpressing a NADPH-GAPDH from *C. acetobutylicum*) strains after shake flask culture under aerobic conditions in LB or 2YT medium supplemented with 20 g/L of glucose for 24 h at 30 °C and 250 rpm. The data shown are the average of three replicate experiments where the error bars represent the standard deviation. Both strains express the pK19-Lyco plasmid containing the genes for lycopene biosynthesis (see Table 1). DCW: dry cell weight.

the mutant strain produced 72.7% more NADPH than the control strain. Also, the product formation rate was almost doubled.

The results of the two model systems showed that the *gapA* mutant *E. coli* strain expressing the NADPH-dependent *gapC* from *C. acetobutylicum* has a higher NADPH availability that the control and can be used to increase the yield and productivity of NADPH-dependent products.

4. Discussion

Many studies have shown that *E. coli* adapts its metabolism by activating/inactivating alternative pathways to reach reducing power balance and efficiently utilize the available nutrients. The inactivation of the NAD-dependent GAPDH gene (*gapA*) and the overexpression of the NADP-dependent GAPDH gene (*gapC*) from *C. acetobutylicum* produced a change in the metabolic flux

Table 3
Production of ε-caprolactone in shake flasks by non-growing NADH-GAPDH *E. coli* mutant strain overexpressing a NADPH-GAPDH from *C. acetobutylicum* using glucose as energy source

Strain	ε-caprolactone volumetric productivity[a] (mmol/l h)	Yield[b] (mol NADPH/mol glucose)
BL21(DE3) pDHC29 pMM_4(control)	2.49 ± 0.18	1.72 ± 0.19
MBS100B pHL621 pMM4 Δ*gapA*⁻*gapC*⁺	4.86 ± 0.16	2.97 ± 0.05

[a] The volumetric productivity was calculated using the total culture volume.
[b] The yield was calculated considering the NAPDH produced that was used for ε-caprolactone biosynthesis. In this experiment the cells are used as reaction catalysts under non-growing conditions. The production of each ε-caprolactone molecule requires one molecule of NADPH.

distribution within the cell. The mutant strain showed a higher flux through glycolysis and a reduced flux through the PP pathway compared to the control. This is a combined effect of the overexpression of the *gapC* gene and the generation of NADPH during glycolysis, alleviating the requirement NADPH provided by the PP pathway. The mutant *E. coli* strain did not show growth deficiency, but on the contrary it grew faster under many of the conditions tested. Kabir and Shimizu (Kabir and Shimizu, 2003a, b) studied an *E. coli* strain where the phosphoglucose isomerase gene (*pgi*) was knocked out to direct the carbon flow through the PP pathway, the main source of NADPH in the cell. But in this case the mutant strain showed growth deficiency. This deficiency was later partially recovered when the PHB synthetic pathway was introduced into the cells. This approach was later complemented by overexpressing the *udhA* gene from *E. coli* encoding for pyridine nucleotide transhydrogenase, an enzyme responsible for the interchange of reducing power between NADH and NADPH, that showed an increase of 25% in cell growth by partially re-establishing the redox equilibrium (Kabir and Shimizu, 2003a).

The overexpression of the NADPH-dependent GAPDH from *C. acetobutylicum* together with the knockout of the native NADH-dependent GAPDH showed improvement in lycopene and ε-caprolactone synthesis confirming that cofactor availability is a limiting factor for the system. In a similar manner, Verho and collaborators showed an increase in the rate and yield of ethanol production from D-xylose by increasing the NADPH availability by the overexpression of a $NADP^+$-GAPDH in *S. cerevisiae* Verho et al. (2003).

Farmer and Liao (2001) manipulated precursor availability to increase lycopene production, they showed the GAP pool could be a limiting factor in their system. Although, that was not the case in our system, the overexpression of GAPDH lead to a higher flux though glycolysis and to a higher conversion of GAP into 3PG virtually making less GAP available for lycopene synthesis but the modification in the glycolysis pathway resulted in an increase of lycopene synthesis likely due to a higher NADPH availability.

As the lycopene and ε-caprolactone production experiments indicated, replacing the NAD^+-dependent GAPDH (*gapA*) with the $NADP^+$-dependent GAPDH (*gapC*) may result in reduced NADH production while producing more NADPH. However, since the chemostat cultures were conducted under aerobic conditions, it is very difficult to explore the impact of reduced NADH production due to variant respiratory chain regulations and P/O ratios. The overproduction of NADPH should also affect the $NADP^+$ availability in the reaction through isocitrate dehydrogenase, which is mainly $NADP^+$-dependent (Dean et al., 1996; Hurley et al., 1991). The slightly higher biomass concentration in the bioreactor will result in a lower oxygen level in the *gapA gapC* strain culture than

that of the wild type strain. Both factors will result in relatively lower TCA cycle fluxes in the *gapA gapC* strain culture than that of the wild type strain. The higher acetate production in the *gapA gapC* strain compared to the control strain could be a consequence of lower TCA cycle fluxes.

The single step reaction for the formation of ε-caprolactone from cyclohexanone catalyzed by resting *E. coli* showed that the mutant strain was able to produce 73% more NADPH than the control.

Each production system involved the construction of a *gapA gapC* strain based on a different *E. coli* host. Different genetic backgrounds in *E. coli* could lead to different culture behaviors (enzyme expression) and therefore different products profiles. In this study we showed that two *E. coli gapA* mutant strains with different backgrounds (MG1655 and BL21(DE3)) exhibited an increase in NADPH-dependent product synthesis when the endogenous NAD^+-GAPDH was replaced by the $NADP^+$-GAPDH from *C. acetobutylicum* showing the flexibility of the approach.

The synthesis of lycopene and ε -caprolactone was increased in the mutant strain to different extents due to differences in synthetic pathways and precursor metabolites. A combination of different strategies where an optimal balance between precursors and cofactors is achieved would lead to higher improvement in product yields.

5. Conclusion

The overexpression of the NADPH-dependent GAPDH from *C. acetobutylicum* together with the knockout of the native NADH-dependent GAPDH successfully increased NADPH availability in two different *E. coli* whole cell-systems, showed by the increase in lycopene and ε-caprolactone productions.

Acknowledgments

This work was supported in part by the National Science Foundation (BES-0420840; CBET-0828516).

Appendix A. Abbreviations in Fig. 3

3PG	3-phosphoglycerate
AcCoA	acetyl-CoA
AKG	α-ketoglutarate
E4P	erythrose 4-phosphate
F6P	fructose-6-phosphate
FDP	fructose 1, 6-diphosphate
FUM	fumarate
GAP	glyceraldehyde 3-phosphate
G6P	glucose-6-phosphate
ICT	isocitrate
Mal	malate
NADH	nicotinamide adenine dinucleotide
NADPH	nicotinamide adenine dinucleotide phosphate
OAA	oxaloacetate
P5P	pentose 5-phosphate
PEP	phosphoenolpyruvate
PYR	pyruvate
S7P	sedo-heptulose 7-phosphate
Suc	succinate

References

Agarwal, S., Rao, A.V., 2000. Tomato lycopene and its role in human health and chronic diseases. CMAJ 163 (6), 739–744.

Alper, H., Stephanopoulos, G., 2008. Uncovering the gene knockout landscape for improved lycopene production in *E. coli*. Appl. Microbiol. Biotechnol. 78 (5), 801–810.

Alper, H., Jin, Y.S., Moxley, J.F., Stephanopoulos, G., 2005. Identifying gene targets for the metabolic engineering of lycopene biosynthesis in *Escherichia coli*. Metab. Eng. 7 (3), 155–164.

Baldwin, C.V., Woodley, J.M., 2006. On oxygen limitation in a whole cell biocatalytic Baeyer–Villiger oxidation process. Biotechnol. Bioeng. 95 (3), 362–369.

Berrios-Rivera, S.J., Bennett, G.N., San, K.Y., 2002a. The effect of increasing NADH availability on the redistribution of metabolic fluxes in *Escherichia coli* chemostat cultures. Metab. Eng. 4 (3), 230–237.

Berrios-Rivera, S.J., Bennett, G.N., San, K.Y., 2002b. Metabolic engineering of *Escherichia coli*: increase of NADH availability by overexpressing an NAD(+)-dependent formate dehydrogenase. Metab. Eng. 4 (3), 217–229.

Berrios-Rivera, S.J., San, K.Y., Bennett, G.N., 2002c. The effect of NAPRTase overexpression on the total levels of NAD, the NADH/NAD+ ratio, and the distribution of metabolites in *Escherichia coli*. Metab. Eng. 4 (3), 238–247.

Berrios-Rivera, S.J., Sanchez, A.M., Bennett, G.N., San, K.Y., 2004. Effect of different levels of NADH availability on metabolite distribution in *Escherichia coli* fermentation in minimal and complex media. Appl. Microbiol. Biotechnol. 65 (4), 426–432.

Bose, K.S., Agrawal, B.K., 2007. Effect of lycopene from cooked tomatoes on serum antioxidant enzymes, lipid peroxidation rate and lipid profile in coronary heart disease. Singapore Med. J. 48 (5), 415–420.

Chen, G., Kayser, M.M., Mihovilovic, M.D., Mrstik, M.E., Martinez, C.A., Stewart, J.D., 1999. Asymmetric oxydations at sulfur catalyzed engineered strains that overexpress cyclohexanone monooxygenase. New J. Chem. 23, 827–832.

Cunningham Jr., F.X., Sun, Z., Chamovitz, D., Hirschberg, J., Gantt, E., 1994. Molecular structure and enzymatic function of lycopene cyclase from the cyanobacterium *synechococcus* sp. strain PCC7942. Plant Cell 6 (8), 1107–1121.

Dean, A.M., Shiau, A.K., Koshland Jr., D.E., 1996. Determinants of performance in the isocitrate dehydrogenase of *Escherichia coli*. Protein Sci 5 (2), 341–347.

Donoghue, N.A., Norris, D.B., Trudgill, P.W., 1976. The purification and properties of cyclohexanone oxygenase from *Nocardia gluberula* CL1 and *Acinetobacter* NCIB 9871. Eur. J. Biochem. 63, 175–192.

Ernst, M., Kaup, B., Muller, M., Bringer-Meyer, S., Sahm, H., 2005. Enantioselective reduction of carbonyl compounds by whole-cell biotransformation, combining a formate dehydrogenase and a (R)-specific alcohol dehydrogenase. Appl. Microbiol. Biotechnol. 66 (6), 629–634.

Farmer, W.R., Liao, J.C., 2001. Precursor balancing for metabolic engineering of lycopene production in *Escherichia coli*. Biotechnol. Prog. 17 (1), 57–61.

Ganter, C., Pluckthun, A., 1990. Glycine to alanine substitutions in helices of glyceraldehyde-3-phosphate dehydrogenase: effects on stability. Biochemistry 29 (40), 9395–9402.

Gunnarsson, N., Eliasson, A., Nielsen, J., 2004. Control of fluxes towards antibiotics and the role of primary metabolism in production of antibiotics. Adv. Biochem. Eng. Biotechnol. 88, 137–178.

Hummel, W., 1997. New alcohol dehydrogenases for the synthesis of chiral compounds. Adv. Biochem. Eng. Biotechnol. 58, 145–184.

Hurley, J.H., Dean, A.M., Koshland Jr., D.E., Stroud, R.M., 1991. Catalytic mechanism of NADP(+)-dependent isocitrate dehydrogenase: implications from the structures of magnesium-isocitrate and $NADP^+$ complexes. Biochemistry 30 (35), 8671–8678.

Iddar, A., Valverde, F., Serrano, A., Soukri, A., 2002. Expression, purification, and characterization of recombinant nonphosphorylating NADP-dependent glyceraldehyde-3-phosphate dehydrogenase from *Clostridium acetobutylicum*. Protein Expres. Purif. 25 (3), 519–526.

Kabir, M.M., Shimizu, K., 2003a. Fermentation characteristics and protein expression patterns in a recombinant *Escherichia coli* mutant lacking phosphoglucose isomerase for poly(3-hydroxybutyrate) production. Appl. Microbiol. Biotechnol. 62 (2–3), 244–255.

Kabir, M.M., Shimizu, K., 2003b. Gene expression patterns for metabolic pathway in *pgi* knockout *Escherichia coli* with and without phb genes based on RT-PCR. J. Biotechnol. 105 (1–2), 11–31.

Kim, S.W., Keasling, J.D., 2001. Metabolic engineering of the nonmevalonate isopentenyl diphosphate synthesis pathway in *Escherichia coli* enhances lycopene production. Biotechnol. Bioeng. 72 (4), 408–415.

Kirschner, A., Altenbuchner, J., Bornscheuer, U.T., 2007. Cloning, expression, and characterization of a Baeyer–Villiger monooxygenase from *Pseudomonas fluorescens* DSM 50106 in *E. coli*. Appl. Microbiol. Biotechnol. 73 (5), 1065–1072.

Kyte, B.G., Rouviere, P., Cheng, Q., Stewart, J.D., 2004. Assessing the substrate selectivities and enantioselectivities of eight novel Baeyer–Villiger monooxygenases toward alkyl-substituted cyclohexanones. J. Org. Chem. 69 (1), 12–17.

Lee, W.N., Bergner, E.A., Guo, Z.K., 1992. Mass isotopomer pattern and precursor–product relationship. Biol. Mass Spectrom. 21 (2), 114–122.

Lee, W.H., Park, Y.C., Lee, D.H., Park, K., Seo, J.H., 2005. Simultaneous biocatalyst production and Baeyer–Villiger oxidation for bioconversion of cyclohexanone by recombinant *Escherichia coli* expressing cyclohexanone monooxygenase. Appl. Biochem. Biotechnol. 121–124, 827–836.

Mihovilovic, M.D., Rudroff, F., Muller, B., Stanetty, P., 2003. First enantiodivergent Baeyer–Villiger oxidation by recombinant whole-cells expressing two monooxygenases from *Brevibacterium*. Bioorg. Med. Chem. Lett. 13 (8), 1479–1482.

Minorsky, P.V., 2002. Lycopene and human health. Plant Physiol. 130 (3), 1077–1078.

Moreira dos Santos, M., Raghevendran, V., Kotter, P., Olsson, L., Nielsen, J., 2004. Manipulation of malic enzyme in *Saccharomyces cerevisiae* for increasing NADPH production capacity aerobically in different cellular compartments. Metab. Eng. 6 (4), 352–363.

Neidhardt, F.C., Ingraham, J.L., Schaechter, M., 1990. Physiology of the Bacterial Cell. A Molecular Approach.
Phillips, G.J., Park, S.K., Huber, D., 2000. High copy number plasmids compatible with commonly used cloning vectors. Biotechniques 28 (3), 400-2, 404, 406 passim.
Pridmore, R.D., 1987. New and versatile cloning vectors with kanamycin-resistance marker. Gene 56 (2–3), 309–312.
Rao, A.V., Agarwal, S., 2000. Role of antioxidant lycopene in cancer and heart disease. J. Am. Coll. Nutr. 19 (5), 563–569.
San, K.Y., Bennett, G.N., Berrios-Rivera, S.J., Vadali, R.V., Yang, Y.T., Horton, E., Rudolph, F.B., Sariyar, B., Blackwood, K., 2002. Metabolic engineering through cofactor manipulation and its effects on metabolic flux redistribution in *Escherichia coli*. Metab. Eng. 4 (2), 182–192.
Sanchez, A.M., Bennett, G.N., San, K.Y., 2005. Novel pathway engineering design of the anaerobic central metabolic pathway in *Escherichia coli* to increase succinate yield and productivity. Metab. Eng. 7 (3), 229–239.
Sanchez, A.M., Andrews, J., Hussein, I., Bennett, G.N., San, K.Y., 2006. Effect of overexpression of a soluble pyridine nucleotide transhydrogenase (UdhA) on the production of poly(3-hydroxybutyrate) in *Escherichia coli*. Biotechnol. Prog. 22 (2), 420–425.
Schmidt, K., Carlsen, M., Nielse, J., Villadsen, J., 1997. Modeling isotopomer distributions in biochemical networks using isotopomer mapping matrices. Biotechnol. Bioeng. 55, 831–840.
Schmidt, K., Norregaard, L.C., Pedersen, B., Meissner, A., Duus, J.O., Nielsen, J.O., Villadsen, J., 1999. Quantification of intracellular metabolic fluxes from fractional enrichment and ^{13}C–^{13}C coupling constraints on the isotopomer distribution in labeled biomass components. Metab. Eng. 1 (2), 166–179.
Schulz, F., Leca, F., Hollmann, F., Reetz, M.T., 2005. Towards practical biocatalytic Baeyer–Villiger reactions: applying a thermostable enzyme in the gram-scale synthesis of optically-active lactones in a two-liquid-phase system. Beilstein J. Org. Chem. 1 (1), 10.
Stacewicz-Sapuntzakis, M., Bowen, P.E., 2005. Role of lycopene and tomato products in prostate health. Biochim. Biophys. Acta 1740 (2), 202–205.
Stephanopoulos, G.N., Aristidou, A.A., Nielsen, J., 1998. Metabolic Engineering: Principles and Methodologies, 327pp.
Stewart, J.D., Reed, K.W., Zhu, J., Chen, G., Kayser, M.M., 1996. A ‘‘designer yeast’’ that catalyzes the kinetic resolutions of 2-alkyl-substituted cyclohexanones by enantioselective Baeyer–Villiger oxidations. J. Org. Chem. 61 (22), 7652–7653.
Szyperski, T., 1995. Biosynthetically directed fractional ^{13}C-labeling of proteinogenic amino acids. An efficient analytical tool to investigate intermediary metabolism. Eur. J. Biochem. 232 (2), 433–448.
Vadali, R.V., Fu, Y., Bennett, G.N., San, K.Y., 2005. Enhanced lycopene productivity by manipulation of carbon flow to isopentenyl diphosphate in *Escherichia coli*. Biotechnol. Prog. 21 (5), 1558–1561.
Van Beilen, J.B., Mourlane, F., Seeger, M.A., Kovac, J., Li, Z., Smits, T.H., Fritsche, U., Witholt, B., 2003. Cloning of Baeyer–Villiger monooxygenases from comamonas, xanthobacter and rhodococcus using polymerase chain reaction with highly degenerate primers. Environ. Microbiol. 5 (3), 174–182.
van Winden, W.A., Wittmann, C., Heinzle, E., Heijnen, J.J., 2002. Correcting mass isotopomer distributions for naturally occurring isotopes. Biotechnol. Bioeng. 80 (4), 477–479.
Verho, R., Richard, P., Jonson, P.H., Sundqvist, L., Londesborough, J., Penttila, M., 2002. Identification of the first fungal NADP-GAPDH from *kluyveromyces lactis*. Biochemistry 41 (46), 13833–13838.
Verho, R., Londesborough, J., Penttila, M., Richard, P., 2003. Engineering redox cofactor regeneration for improved pentose fermentation in *Saccharomyces cerevisiae*. Appl. Environ. Microbiol. 69 (10), 5892–5897.
Walton, A.Z., Stewart, J.D., 2002. An efficient enzymatic Baeyer–Villiger oxidation by engineered *Escherichia coli* cells under non-growing conditions. Biotechnol. Prog. 18 (2), 262–268.
Walton, A.Z., Stewart, J.D., 2004. Understanding and improving NADPH-dependent reactions by nongrowing *Escherichia coli* cells. Biotechnol. Prog. 20 (2), 403–411.
Wiechert, W., de Graaf, A.A., 1997. Bidirectional reaction steps in metabolic engineering networks: I. Modeling and simulation of carbon isotope labeling experiments. Biotechnol. Bioeng. 55, 101–117.
Wiechert, W., Siefke, C., De Graaf, A.A., Marx, A., 1997. Bidirectional reaction steps in metabolic networks: II flux estimation and statistical analysis. Biotechnol. Bioeng. 55, 118–135.
Yang, Y.T., San, K.Y., Bennett, G.N., 1999. Redistribution of metabolic fluxes in *Escherichia coli* with fermentative lactate dehydrogenase overexpression and deletion. Metab. Eng. 1 (2), 141–152.
Zhao, J., Shimizu, K., 2003. Metabolic flux analysis of *Escherichia coli* K12 grown on ^{13}C-labeled acetate and glucose using GC-MS and powerful flux calculation method. J. Biotechnol. 101 (2), 101–117.
Zhu, J., Shalel-Levanon, S., Bennett, G., San, K.Y., 2006. Effect of the global redox sensing/regulation networks on *Escherichia coli* and metabolic flux distribution based on C-13 labeling experiments. Metab. Eng. 8 (6), 619–627.
Zupke, C., Stephanopoulos, G., 1994. Modeling of isotope distributions and intracellular fluxes in metabolic networks using atom mapping matrices. Biotechnol. Prog. 10, 489–498.